

Graph Neural Networks for Maximum Constraint Satisfaction

Jan Toenshoff

Martin Ritzert

Hinrikus Wolf

Martin Grohe

February 12, 2020
RWTH Aachen University

Many combinatorial optimization problems can be phrased in the language of constraint satisfaction problems. We introduce a graph neural network architecture for solving such optimization problems. The architecture is generic; it works for all binary constraint satisfaction problems. Training is unsupervised, and it is sufficient to train on relatively small instances; the resulting networks perform well on much larger instances (at least 10-times larger). We experimentally evaluate our approach for a variety of problems, including Maximum Cut and Maximum Independent Set. Despite being generic, we show that our approach matches or surpasses most greedy and semi-definite programming based algorithms and sometimes even outperforms state-of-the-art heuristics for the specific problems.

1. Introduction

Constraint satisfaction is a general framework for casting combinatorial search and optimization problems; many well-known NP-complete problems, for example, k -colorability, Boolean satisfiability and maximum cut can be modeled as constraint satisfaction problems (CSPs). Our focus is on the optimization version of constraint satisfaction, usually referred to as maximum constraint satisfaction (MAX-CSP), where the objective is to satisfy as many constraints of a given instance as possible. There is a long tradition of designing exact and heuristic algorithms for all kinds of CSPs. Our work should be seen in the context of a recently renewed interest in heuristics for NP-hard combinatorial problems based on neural networks, mostly graph neural networks (for example, (Lemos et al. 2019; Prates et al. 2019; Selsam et al. 2019)).

We present a generic graph neural network (GNN) based architecture called RUN-CSP (Recurrent Unsupervised Neural Network for Constraint Satisfaction Problems) with the following key features:

Unsupervised: Training is completely unsupervised and just requires a set of instances of the problem.

Scalable: Networks trained on small instances achieve good results on much larger inputs.

Generic: The architecture is generic and can learn to find approximate solutions for any binary MAX-CSP.

We focus on binary CSPs, where each constraint involves only two variables. This is no severe restriction, because every CSP can be transformed into an equivalent binary CSP (see (Dechter 2003)).

To solve MAX-CSPs, we train a graph neural network which we view as a message passing protocol. The protocol is executed on a graph with nodes for all variables of the instance and edges for all constraints. Associated with each node are two states, a short-term state and a long-term state, which are both vectors of some fixed length. The exchanged messages are linear functions of the short-term states. We update the internal states using an LSTM (Long Short-Term Memory) cell for each variable and share the parameters of the internal functions over all variables. Finally, we extract probabilities for the possible values of each variable from its short-term state through a linear function combined with softmax activation. The parameters of the LSTM, message generation, and readout function are learned. Since all parameters are shared over all variables, we can apply the model to instances of arbitrary size¹.

For training, we design a loss function that rewards solutions with many satisfied constraints. Effectively, through the choice of the loss function, we train our networks to satisfy the maximum number of constraints. Our focus on the optimization problem MAX-CSP rather than the decision problem allows us to train unsupervised. This is a major point of distinction between our work and recent neural approaches to Boolean satisfiability (Selsam et al. 2019) and the coloring problem (Lemos et al. 2019). Both approaches require supervised training and output a prediction for satisfiability or coloring number. In contrast, our framework returns an (approximately optimal) variable assignment.

We experimentally evaluate our approach on the following NP-hard problems: the maximum 2-satisfiability problem (MAX-2-SAT), which asks for an assignment maximizing the number of satisfied clauses for a given Boolean formula in 2-conjunctive normal form; the maximum cut problem (MAX-CUT), which asks for a partition of a graph in two parts such that the number of edges between the parts is maximal (see Figure 1); the 3-colorability problem (3-COL), which asks for a 3-coloring of the vertices of a given graph such that the two endvertices of each edge have distinct colors. We also consider the maximum independent set problem MAX-IS, which asks for an independent set of maximum cardinality in a given graph. Strictly speaking, MAX-IS is not a maximum constraint satisfaction problem, because its objective is not to maximize the number of satisfied constraints, but to satisfy all constraints while maximizing the number of variables with a certain value. We include this problem to demonstrate that our approach can easily be adapted to such related problems.

¹Our Tensorflow implementation of RUN-CSP is available at <https://github.com/RUNCSP/RUN-CSP>.

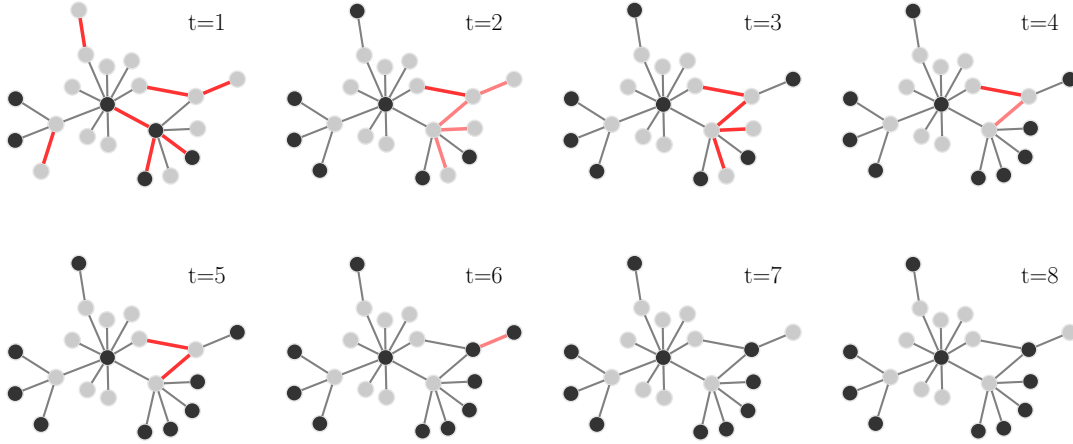


Figure 1: A maximum cut for a graph found by RUN-CSP in seven iterations. Edges not part of the cut are shown in red.

We demonstrate that our simple generic approach works well for all four problems and matches competitive baselines. Since our approach is generic for all MAX-CSPs, those baselines include other general approaches such as greedy algorithms and semi-definite programming (SDP). The latter is particularly relevant, because it is known (under certain complexity theoretic assumptions) that SDP achieves optimal approximation ratios for all MAX-CSPs (Raghavendra 2008). For MAX-2-SAT, our approach even manages to surpass a state-of-the-art heuristic.

Almost all models are trained on quite small training sets consisting of small random instances. We evaluate those models on unstructured random instances as well as highly structured benchmark instances. Instance sizes vary from small instances with 100 variables and 200 constraints to medium sized instances with more than 1,000 variables and over 10,000 constraints. We observe that RUN-CSP is able to generalize well from small instances to instances both smaller and much larger. The largest (benchmark) instance we evaluate on has approximately 120,000 constraints, but that instance required the use of large training graphs. Computations with RUN-CSP are very fast in comparison to many heuristics and profits from modern hardware like GPUs. For medium-sized instances with 10,000 constraints the computation takes less than five seconds.

We do not claim that our method is in general competitive with state-of-the-art heuristics for specific problems. Furthermore, it has to be distinguished from solvers which in addition to a solution return a guarantee that no better solution exists. However, we demonstrate that our approach clearly improves on the state-of-the-art for neural methods on small and medium-sized binary CSP instances, while still being completely generic.

1.1. Related Work

An early group of papers dates back to the 1980’s and uses Hopfield Networks (Hopfield and Tank 1985) to approximate TSP and other discrete problems using neural networks. Hopfield and Tank use a single-layer neural network with sigmoid activation and apply gradient descent to come up with an approximative solution. The loss function adopts soft assignments and uses the length of the TSP tour and a term penalizing incorrect tours as loss, hence being unsupervised. This approach has been extended to k -colorability (Dahl 1987; Gassen and Carothers 1993; Harmanani, Hannouche, and Khoury 2010; Takefuji and Lee 1991) and other CSPs (Adorf and Johnston 1990). The loss functions used in some of these approaches are similar to ours.

Newer approaches involve modern machine learning techniques and are usually based on graph neural networks (GNNs). NeuroSAT (Selsam et al. 2019), a learned message passing network for predicting satisfiability, reignited the interest in solving NP-complete problems with neural networks. Prates et al. (2019) use GNNs to learn TSP trained on instances of the form $(G, \ell \pm \varepsilon)$ where ℓ is the length of an optimal tour on G . They achieved good results on graphs with up to 40 nodes. Using the same idea, Lemos et al. (2019) learned to predict k -colorability of graphs scaling to larger graphs and chromatic numbers than seen during training. Yao, Bandeira, and Villar (2019) evaluated the performance of unsupervised GNNs for the MAX-CUT problem. They adapted a GNN architecture by Chen, Li, and Bruna (2019) to MAX-CUT and trained two versions of their network, one through policy gradient descent and the other via a differentiable relaxation of the loss function which both achieved similar results. Amizadeh, Matusevych, and Weimer (2019) proposed an unsupervised architecture for CIRCUIT-SAT, which predicts satisfying variable assignments for a given formula. For the #P-hard weighted model counting problem for DNF formulas, Abboud, Ceylan, and Lukasiewicz (2019) applied a GNN-based message passing approach. For large instances with more than 100,000 nodes, Li, Chen, and Koltun (2018) use a GNN to guide a tree search for MAX-IS and Khalil et al. (2017) choose the best heuristic for TSP through reinforcement learning.

2. Method

In this section, we describe our RUN-CSP architecture for MAX-CSPs. Formally, a CSP-instance is a triple $I = (X, D, C)$, where X is a set of variables, D is a domain, and C is a set of constraints of the form (x_1, \dots, x_ℓ, R) for some $R \subseteq D^\ell$. We only consider binary constraints (with $\ell = 2$) in this paper. A *constraint language* is a finite set Γ of relations over some fixed domain D , and I is a Γ -instance if $R \in \Gamma$ for all constraints $(x_1, x_2, R) \in C$. An *assignment* $\alpha : X \rightarrow D$ satisfies a constraint (x_1, x_2, R) if $(\alpha(x_1), \alpha(x_2)) \in R$, and it satisfies the instance I if it satisfies all constraints in C . CSP(Γ) is the problem of deciding whether a given Γ -instance has a satisfying assignment and finding such an assignment if there is one. MAX-CSP(Γ) is the problem of finding an assignment that satisfies the maximum number of constraints.

For example, an instance of 3-COL has a variable x_v for each vertex v of the input graph, domain $D = \{1, 2, 3\}$, and a constraint (v, w, R_{\neq}^3) for each edge vw of the graph.

Here $R_{\neq}^3 = \{(1, 2), (2, 1), (1, 3), (3, 1), (2, 3), (3, 2)\}$ is the inequality relation on $\{1, 2, 3\}$. Thus 3-COL is $\text{CSP}(\{R_{\neq}^3\})$.

2.1. Architecture

We use a randomized recurrent graph neural network architecture to evaluate a given problem instance using message passing. For any binary constraint language Γ a RUN-CSP network can be trained to approximate $\text{MAX-CSP}(\Gamma)$. Intuitively, our network can be viewed as a trainable communication protocol through which the variables of a given instance can negotiate a value assignment. With every variable $x \in X$ we associate a short-term state $s_x^{(t)} \in \mathbb{R}^k$ and a hidden (long-term) state $h_x^{(t)} \in \mathbb{R}^k$ which change throughout the message passing iterations $t \in \{0, \dots, t_{\max}\}$. The short-term state vector $s_x^{(0)}$ for every variable x is initialized by sampling each value independently from a normal distribution with zero mean and unit variance. All hidden states $h_x^{(0)}$ are initialized as zero vectors.

Every message passing step uses the same weights and thus we are free to choose the number $t_{\max} \in \mathbb{N}$ of iterations for which RUN-CSP runs on a given problem instance. This number may or may not be identical to the number of iterations used for training. The state size k and the number of iterations used for training t_{\max}^{tr} and evaluation t_{\max}^{ev} are the main hyperparameters of our network.

Variables x and y that co-occur in a constraint $c = (x, y, R)$ can exchange messages. Each message depends on the states $s_x^{(t)}, s_y^{(t)}$, the relation R and the order of x and y in the constraint, but not the internal long-term states $h_x^{(t)}, h_y^{(t)}$. The dependence on R allows the network to send different messages whenever the states of x and y correspond to a satisfying or unsatisfying assignment for each constraint. This dependence implies that we have independent message generation functions for every relation R in the constraint language Γ . We therefore require Γ to be fixed. The process of message passing and updating the internal states is repeated t_{\max} times. We use linear functions to compute the messages. (Experiments showed that more complicated functions did not improve performance while being less stable and less efficient during training.) Thus, the messaging function for every relation R is defined by a trainable weight matrix $M_R \in \mathbb{R}^{2k \times 2k}$ as

$$S_R \left(s_x^{(t)}, s_y^{(t)} \right) = M_R \begin{pmatrix} s_x^{(t)} \\ s_y^{(t)} \end{pmatrix}. \quad (1)$$

The output of S_R are two stacked k -dimensional vectors, which represent the messages to x and y , respectively. Since M_R is in general not symmetric, the generated messages depend on the order of the variables in the constraint. This behavior is desirable for asymmetric relations. For symmetric relations we modify S_R to produce messages independently from the order of variables in c . In this case we use a smaller weight matrix $M_R \in \mathbb{R}^{2k \times k}$ to generate both messages:

$$S_R(s_x^{(t)}, s_y^{(t)}) = \left(M_R \begin{pmatrix} s_x^{(t)} \\ s_y^{(t)} \end{pmatrix}, M_R \begin{pmatrix} s_y^{(t)} \\ s_x^{(t)} \end{pmatrix} \right)$$

The two messages can still be different, but the content of each message depends only on the states of the endpoints.

The internal states h_x and s_x are updated by an LSTM cell based on the mean of the received messages. For a variable x which received the messages m_1, \dots, m_ℓ the new states are thus computed by

$$h_x^{(t+1)}, s_x^{(t+1)} = \text{LSTM}\left(h_x^{(t)}, s_x^{(t)}, \frac{1}{\ell} \sum_{i=1}^{\ell} m_i\right). \quad (2)$$

For every variable x and iteration $t \in \{1, \dots, t_{\max}\}$ the network produces a soft assignment $\varphi^{(t)}(x)$ from the state $s_x^{(t)}$. In our architecture we use $\varphi^{(t)}(x) = \text{softmax}(W s_x^{(t)})$ with $W \in \mathbb{R}^{d \times k}$ trainable and $d = |D|$. In φ , the linear function reduces the dimensionality while the softmax function enforces stochasticity. The soft assignments $\varphi^{(t)}(x)$ can be interpreted as probabilities of a variable x receiving a certain value $v \in D$. If the domain D contains only two values, we compute a ‘probability’ $p^{(t)}(x) = \sigma(W s_x^{(t)})$ for each node with $W \in \mathbb{R}^{1 \times k}$. The soft assignment is then given by $\varphi^{(t)}(x) = (p^{(t)}(x), 1 - p^{(t)}(x))$. To obtain a hard variable assignment $\alpha^{(t)} : X \rightarrow D$, we assign the value with the highest estimated probability in $\varphi^{(t)}(x)$ for each variable $x \in X$. We select the hard assignment with the most satisfied constraints as the final prediction of the network. This is not necessarily $\alpha^{(t_{\max}^{\text{ev}})}$.

Algorithm 1 describes the architecture in pseudocode. Note that the network’s output depends on the random initialization of the short-term states $s_x^{(0)}$. Those states are the basis for all messages sent during inference and thus for the solution found by RUN-CSP. By applying the network multiple times to the same input and choosing the best solution, we can therefore boost the performance.

2.2. Loss Function

In the following we derive our loss function used for unsupervised training. Let $I = (X, D, C)$ be a CSP-instance. Assume without loss of generality that $D = \{1, \dots, d\}$ for a positive integer d . Given I , in every iteration our network will produce a soft variable assignment $\varphi : X \rightarrow [0, 1]^d$, where $\varphi(x)$ is stochastic for every $x \in X$. Instead of choosing the value with the maximum probability in $\varphi(x)$, we could obtain a hard assignment $\alpha : X \rightarrow D$ by independently sampling a value for each $x \in X$ from the distribution specified by $\varphi(x)$. In this case, the probability that any given constraint $(x, y, R) \in C$ is satisfied by α can be expressed by

$$\Pr_{\alpha \sim \varphi} [(\alpha(x), \alpha(y)) \in R] = \varphi(x)^T A_R \varphi(y) \quad (3)$$

where $A_R \in \{0, 1\}^{d \times d}$ is the characteristic matrix of the relation R with $(A_R)_{i,j} = 1 \iff (i, j) \in R$. We then aim to minimize the combined negative log-likelihood over all constraints:

$$\mathcal{L}_{\text{CSP}}(\varphi, I) := \frac{1}{|C|} \cdot \sum_{(x,y,R) \in C} -\log(\varphi(x)^T A_R \varphi(y)) \quad (4)$$

Algorithm 1: Network Architecture

Input: Instance (X, C) , $t_{\max} \in \mathbb{N}$
Output: $(\varphi^{(1)}, \dots, \varphi^{(t_{\max})}), \varphi^{(t)} : X \rightarrow [0, 1]^d$
for $x \in X$ **do**
 // random initialization
 $s_x^{(0)} \sim \mathcal{N}(0, 1)^k$
 $h_x^{(0)} := \mathbf{0} \in \mathbb{R}^k$
 for $t \in \{1, \dots, t_{\max}\}$ **do**
 for $c := (x, y, R) \in C$ **do**
 // generate messages
 $(m_{c,x}^{(t)}, m_{c,y}^{(t)}) := S_R(s_x^{(t-1)}, s_y^{(t-1)})$
 for $x \in X$ **do**
 // combine messages and update
 $r_x^{(t)} := \frac{1}{\deg(x)} \sum_{c \in C, x \in c} m_{c,x}^{(t)}$
 $(h_x^{(t)}, s_x^{(t)}) := \text{LSTM}(h_x^{(t-1)}, s_x^{(t-1)}, r_x^{(t)})$
 $\varphi^{(t)}(x) := \text{softmax}(W \cdot s_x^{(t)})$

We combine the loss function \mathcal{L}_{CSP} throughout all iterations with a discount factor $\lambda \in [0, 1]$ to get our training objective:

$$\mathcal{L}(\{\varphi_t\}_{t \leq t_{\max}^{\text{tr}}}, I) := \sum_{t=1}^{t_{\max}^{\text{tr}}} \lambda^{t_{\max}^{\text{tr}}-t} \cdot \mathcal{L}_{\text{CSP}}(\varphi^{(t)}, I) \quad (5)$$

This loss function allows us to train unsupervised since it does not depend on any ground truth assignments. In general, computing optimal solutions for supervised training can easily turn out to be prohibitive; our approach completely avoids such computations.

Remarks:

(1) In this paper, we focus on binary CSPs. For the extension to ℓ -ary CSPs for some $\ell \geq 3$ (for example 3-SAT), we note that the generalization of the loss function is straightforward. Exploring network architectures that can process constraints of higher arity remains future work.

(2) It is also possible to extend the framework to the weighted MAX-CSPs where a weight is associated with each constraint. To achieve this, we can replace the averages in the loss function and message collection steps by weighted averages. Early experiments in that direction show promising results.

3. Experiments

To validate our method empirically, we performed experiments for MAX-2-SAT, MAX-CUT, 3-COL and MAX-IS. For all experiments, we used internal states of size $k = 128$; state sizes up to $k = 1024$ did not increase performance for the tested instances. We

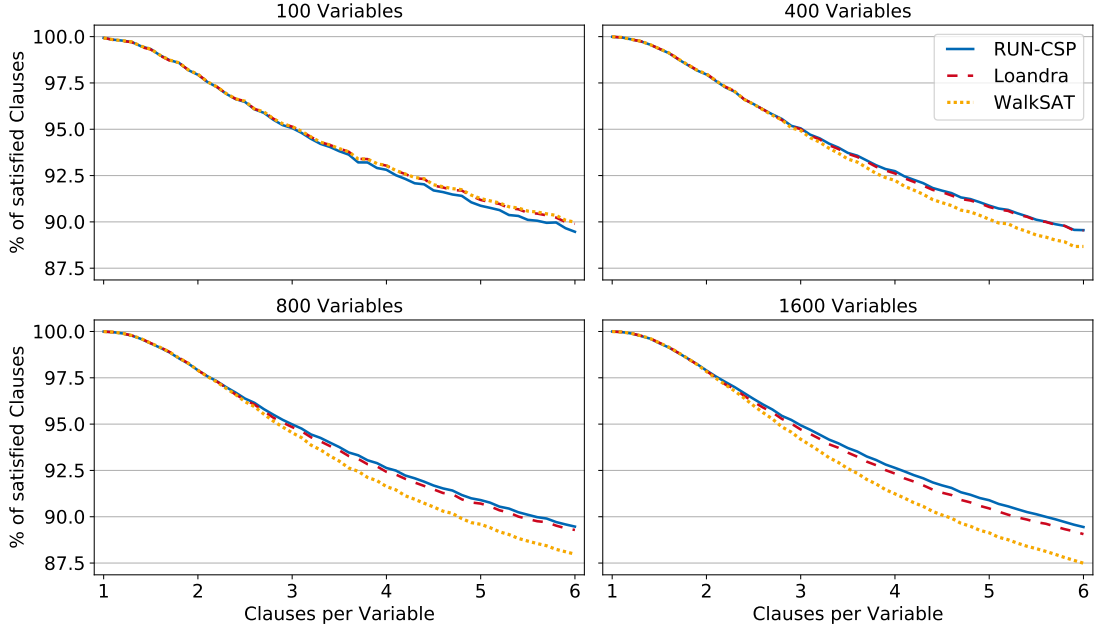


Figure 2: Percentage of satisfied clauses of random 2-CNF formulas for RUN-CSP, Loandra and WalkSAT. Each data point is the average of 100 formulas; the ratio of clauses per variable increases in steps of 0.1.

empirically chose to use $t_{\max}^{\text{tr}} = 30$ iterations during training and, unless stated otherwise, $t_{\max}^{\text{ev}} = 100$ for evaluation. Especially for larger instances it proved beneficial to use a relatively high t_{\max}^{ev} . In contrast, choosing t_{\max}^{tr} too large during training ($t_{\max}^{\text{tr}} > 50$) resulted in unstable training. During evaluation, we use 64 parallel runs for each instance and use the best result. Further increasing this number mainly increases the runtime but has no real effect on the quality of solutions. We trained most models with 4,000 instances split into in 400 batches. Training is performed for 25 epochs using the Adam optimizer with default parameters and gradient clipping at a norm of 1.0. The decay over time in our loss function was set to $\lambda = 0.95$. We provide a more detailed overview of our implementation and training configuration in the appendix.

We ran our experiments on machines with two Intel Xeon 8160 CPUs and one NVIDIA Tesla V100 GPU but got very similar runtimes on consumer hardware. Evaluating 64 runs on an instance with 1,000 variables and 1,000 constraints takes about 1.5 seconds, 10,000 constraints about 5 seconds, and 20,000 constraints about 8 seconds. Training a model takes less than 30 minutes. Thus, the computational cost of RUN-CSP is relatively low.

Table 1: Number of unsatisfied constraints for MAX-2-SAT benchmark instances derived from the Ising spin glass problem. Best solutions are printed in bold.

Instance	$ V $	$ C $	Opt.	RUN-CSP	WalkSAT	Loandra
t3pm3	27	162	17	17	17	17
t4pm3	64	384	38	40	38	38
t5pm3	125	750	78	78	78	78
t6pm3	216	1269	136	136	142	142
t7pm3	343	2058	209	216	227	225

3.1. Max-2-SAT

We view MAX-2-SAT as a binary CSP with domain $D = \{0, 1\}$ and a constraint language consisting of three relations R_{00} (for clauses with two negated literals), R_{01} (one negated literal) and R_{11} (no negated literals). For example, $R_{01} = \{(0, 0), (0, 1), (1, 1)\}$ is the set of satisfying assignments for a clause $(\neg x \vee y)$. For training a RUN-CSP model we used 4,000 random 2-CNF formulas with 100 variables each. The number of clauses was sampled uniformly between 100 and 600 for every formula and each clause was generated by sampling two distinct variables and then independently negating the literals with probability 0.5.

For the evaluation of RUN-CSP in MAX-2-SAT we start with random instances and compare it to a number of problem-specific heuristics. All baselines can solve MAX-SAT for arbitrary arities, not only MAX-2-SAT, while RUN-CSP can solve a variety of binary MAX-CSPs. The state-of-the-art MAX-SAT Solver *Loandra* (Berg, Demirović, and Stuckey 2019) won the unweighted track for incomplete solvers in the MAX-SAT Evaluation 2019 (Bacchus, Järvisalo, and Martins 2019). We ran *Loandra* in its default configuration with a timeout of 20 minutes on each formula. To put this into context, on the largest evaluation instance used here (9,600 constraints) RUN-CSP takes less than seven minutes on a single CPU core and about five seconds using the GPU. *WalkSAT* (Kautz 2019; Selman, Kautz, Cohen, et al. 1993) is a stochastic local search algorithm for approximating MAX-SAT. We allowed WalkSAT to perform 10 million flips on each formula using its ‘noise’ strategy with parameters $n = 2$ and $m = 2000$. Its performance was boosted similarly to RUN-CSP by performing 64 runs and selecting the best result.

For evaluation we generated random formulas with 100, 400, 800 and 1,600 variables. The ratio between clauses and variables was varied in steps of 0.1 from 1 to 6. Figure 2 shows the average percentage of satisfied clauses in the solutions found by each method over 100 formulas for each size and density. The methods yield virtually identical results for formulas with less than 2 clauses per variable. For denser instances, RUN-CSP yields slightly worse results than both baselines when only 100 variables are present. However, it matches the results of *Loandra* for formulas with 400 variables and outperforms the solver for instances with 800 and 1,600 variables. The performance of WalkSAT degrades on these formulas and is significantly worse than RUN-CSP.

For more structured formulas, we use MAX-2-SAT benchmark instances from the

Table 2: P -values of graph cuts produced by RUN-CSP, Yao, SDP, and EO for regular graphs with 500 nodes and varying degrees. We report the mean across 1000 random graphs for each degree.

d	RUN-CSP	Yao Rel.	Yao Pol.	SDP	EO
3	0.714	0.707	0.693	0.702	0.727
5	0.726	0.701	0.668	0.690	0.737
10	0.710	0.670	0.599	0.682	0.735
15	0.697	0.607	0.629	0.678	0.736
20	0.685	0.614	0.626	0.674	0.732

unweighted track of the MAX-SAT Evaluation 2016 (Argelich 2016) based on the Ising spin glass problem (De Simone et al. 1995; Heras et al. 2008). We used the same general setup as in the previous experiment but increased the timeout for Loandra to 60 minutes. In particular we use the same RUN-CSP model trained entirely on random formulas. Table 1 contains the achieved numbers of unsatisfied constraints across the benchmark instances. All methods produced optimal results on the first and the third instance. RUN-CSP slightly deviates from the optimum on the second instance. For the fourth instance RUN-CSP found an optimal solution while both WalkSAT and Loandra did not. On the largest benchmark formula, RUN-CSP again produced the best result.

Thus, RUN-CSP is competitive for random as well as spin-glass-based structured MAX-2-SAT instances. Especially on larger instances it also outperforms conventional methods. Furthermore, training on random instances generalized well to the structured spin-glass instances.

3.2. Max Cut

MAX-CUT is a classical MAX-CSP with only one relation $\{(0,1), (1,0)\}$ used in the constraints. In this section we evaluate RUN-CSP’s performance on this problem. Yao, Bandeira, and Villar (2019) proposed two unsupervised GNN architectures for MAX-CUT. One was trained through policy gradient descent on a non-differentiable loss function while the other used a differentiable relaxation of this loss. They evaluated their architectures on random regular graphs, where the asymptotic MAX-CUT optimum is known. We use their results as well as their baseline results for Extremal Optimization (EO) (Boettcher and Percus 2001) and a classical approach based on semi-definite programming (SDP) (Goemans and Williamson 1995) as baselines for RUN-CSP. To evaluate the sizes of graph cuts Yao, Bandeira, and Villar (2019) introduced a relative performance measure called P -value given by $P(z) = \frac{z/n-d/4}{\sqrt{d/4}}$ where z is the predicted cut size for a d -regular graph with n nodes. Based on results of Dembo, Montanari, Sen, et al. (2017), they showed that the expected P -value of d -regular graphs approaches $P^* \approx 0.7632$ as $n \rightarrow \infty$. P -values close to P^* indicate a cut where the size is close to the expected optimum and larger values are better. While Yao, Bandeira, and Villar trained one instance of their

Table 3: Achieved cut sizes on Gset instances for RUN-CSP, DSDP and BLS.

Graph	$ V $	$ E $	RUN-CSP	DSDP	BLS
G14	800	4694	2943	2922	3064
G15	800	4661	2928	2938	3050
G22	2000	19990	13028	12960	13359
G49	3000	6000	6000	6000	6000
G50	3000	6000	5880	5880	5880
G55	5000	12468	10116	9960	10294

GNN for each tested degree, we trained one network model on 4,000 Erdős-Rényi graphs and applied it to all graphs. For training, each graph had a node count of $n = 100$ and a uniformly sampled number of edges $m \sim U(100, 2000)$. Thus, the model was not trained specifically for regular graphs. Table 2 reports the mean P -values across 1,000 random regular graphs with 500 nodes for different degrees. For every method other than RUN-CSP, we provide the values as reported by Yao, Bandeira, and Villar. While RUN-CSP does not match the cut sizes produced by extremal optimization, it clearly outperforms both versions of the GNN as well as the classical SDP-based approach.

We performed additional experiments on standard MAX-CUT benchmark instances. The Gset dataset (Ye 2003) is a set of 71 weighted and unweighted graphs that are commonly used for testing MAX-CUT algorithms. The dataset contains three different types of random graphs. Those graphs are Erdős-Rényi graphs with uniform edge probability, graphs where the connectivity gradually decays from node 1 to n , and 4-regular toroidal graphs. Here, we use two unweighted graphs for each type from this dataset.

We reused the RUN-CSP model from the previous experiment but increased the number of iterations for evaluation to $t_{\max}^{\text{ev}} = 500$. Our first baseline by Choi and Ye (2000) uses an SDP solver based on dual scaling (DSDP) and a reduction based on the approach of Goemans and Williamson (1995). Our second baseline Breakout Local Search (BLS) is based on the combination of local search and adaptive perturbation (Benlic and Hao 2013). Its results are among the best known solutions for the Gset dataset. For DSDP and BLS we report the values as provided in the literature. Table 8 reports the achieved cut sizes for RUN-CSP, DSDP, and BLS. On G14 and G15, which are random graphs with decaying node degree, the graph cuts produced by RUN-CSP are similar in size to those reported for DSDP. For the Erdős-Rényi graphs G22 and G55 RUN-CSP performs better than DSDP but worse than BLS. Lastly, on the toroidal graphs G49 and G50 all three methods achieved the best known cut size. This reaffirms the observation that our architecture works particularly well for regular graphs. Although RUN-CSP did not outperform the state-of-the-art heuristic in this experiment it performed at least as well as the SDP based approach DSDP.

Table 4: Percentages of hard instances classified correctly by RUN-CSP, Greedy, HybridEA, and GNN-GCP. We evaluate on 1,000 instances for each size. We provide mean and standard deviation across five different RUN-CSP models.

Nodes	RUN-CSP	Greedy	HybridEA	GNN-GCP	
	Pos.	Pos.	Pos.	Pos.	Neg.
50	98.4 ± 0.3	34.0	100.0	77.6	27.0
100	62.5 ± 2.7	6.7	100.0	64.5	37.8
150	15.5 ± 2.3	1.5	98.7	57.7	43.5
200	2.6 ± 0.4	0.5	88.9	51.9	45.3
300	0.1 ± 0.0	0.0	39.9	48.8	52.7
400	0.0 ± 0.0	0.0	15.3	46.3	54.7

3.3. Coloring

Within coloring we focus on the case of 3 colors, i.e. we consider CSPs over the domain $\{1, 2, 3\}$ with one constraint relation $\{(i, j); i, j \in D, i \neq j\}$. In general, RUN-CSP aims to satisfy as many constraints as possible and therefore approximates MAX-3-COL. Instead of evaluating on MAX-3-COL, we evaluate on its practically more relevant decision variant 3-COL which asks whether a given graph is 3-colorable without conflicts. We turn RUN-CSP into a classifier by predicting that a given input graph is 3-colorable if and only if it is able to find a conflict-free vertex coloring.

We evaluate RUN-CSP on so-called ‘hard’ random instances, similar to those defined by Lemos et al. (2019). These instances are a special subclass of Erdős-Rényi graphs where an additional edge can make the graph no longer 3-colorable. We describe our exact generation procedure in the appendix. We trained five RUN-CSP models on 4,000 hard 3-colorable instances with 100 nodes each. In Table 10 we present results for RUN-CSP, a greedy heuristic with DSatur strategy (Brélaz 1979), the state-of-the-art heuristic HybridEA (Galinier and Hao 1999; Lewis 2015; Lewis et al. 2012), and GNN-GCP (Lemos et al. 2019). We trained a GNN-GCP network on the training instances of Lemos et al. (2019) and allowed HybridEA to make 500 million constraint checks on each graph. All algorithms but GNN-GCP report a graph a 3-colorable only if they found a valid 3-coloring on it and thus never produce false positives. Thus, we additionally report values for GNN-GCP on the non-3-colorable counterparts of the evaluation instances. For GNN-GCP we observe that it roughly gets the chromatic number right and only predicts 3 or 4 on our test graphs. Nevertheless, it seems unable to correctly classify the test instances as high accuracy on positive instances comes with low accuracy on negative instances and vice versa. For the other three algorithms we observe a clear hierarchy. HybridEA expectedly performs best and finds solutions even for some of the largest graphs. RUN-CSP correctly classifies most of the graphs up to 100 nodes and clearly outperforms GNN-GCP. The weakest algorithm is DSatur which even fails on most of the small 50 node graphs.

Using a RUN-CSP model trained on a mixture of random graphs performs slightly

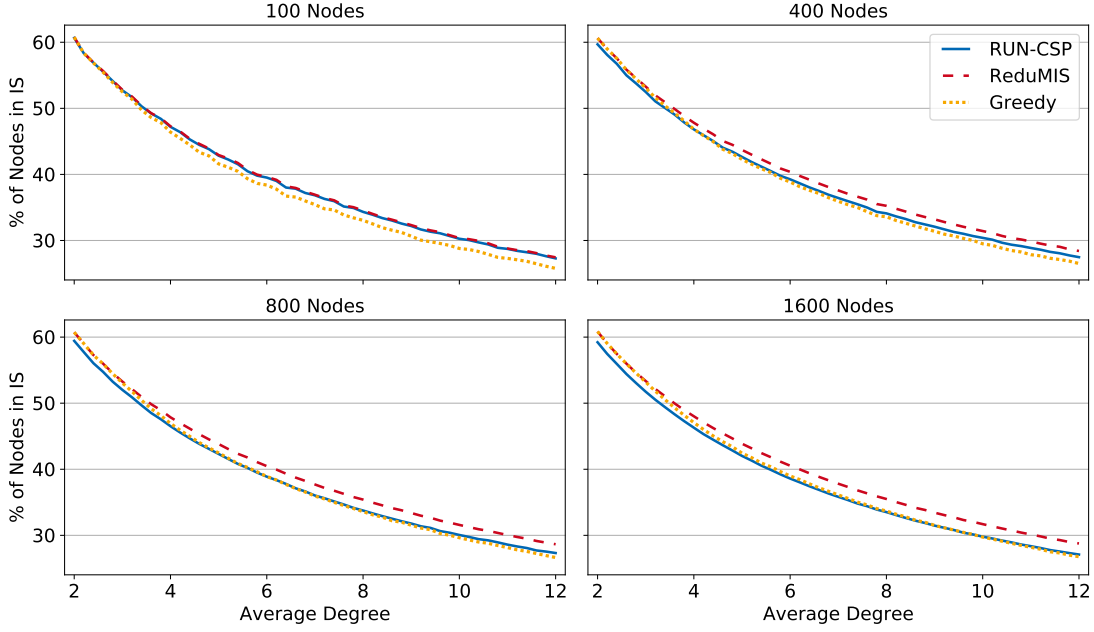


Figure 3: Independent set sizes on random graphs produced by RUN-CSP, ReduMIS and a greedy heuristic. The sizes are given as the percentage of nodes contained in the independent set. Every data point is the average for 100 graphs; the degree increases in steps of 0.2.

worse than models trained on hard random graphs only (shown in the appendix).

Overall, we see that despite being designed for maximization tasks, RUN-CSP outperforms greedy heuristics and neural baselines on the decision variant of 3-COL for hard random instances.

3.4. Independent Set

Finally, we experimented with the maximum independent set problem MAX-IS. The independence condition can be modeled through a constraint language Γ_{IS} with one binary relation $R_{\text{IS}} = \{(0,0), (0,1), (1,0)\}$. Here, assigning the value 1 to a variable is equivalent to including the corresponding node in the independent set. MAX-IS is *not* simply MAX-CSP(Γ_{IS}), since the empty set will trivially satisfy all constraints. Instead, MAX-IS is equivalent to finding an assignment which satisfies R_{IS} at all edges while maximizing an additional objective function that measures the size of the independent set. To model this in our framework, we extend the loss function to reward assignments with many variables set to 1. For a graph $G = (V, E)$ and a soft assignment $\varphi : V \rightarrow [0, 1]$, we define

$$\begin{aligned} \mathcal{L}_{\text{MIS}}(\varphi, G) &= (\kappa + \mathcal{L}_{\text{CSP}}(\varphi, G)) \cdot (1 + \mathcal{L}_{\text{size}}(\varphi, G)), \\ \mathcal{L}_{\text{size}}(\varphi, G) &= \frac{1}{|V|} \sum_{v \in V} (1 - \varphi(v)). \end{aligned} \tag{6}$$

Here, \mathcal{L}_{CSP} is the standard RUN-CSP loss for Γ_{IS} and κ adjusts the relative importance of \mathcal{L}_{CSP} and $\mathcal{L}_{\text{size}}$. Intuitively, smaller values for κ decrease the importance of $\mathcal{L}_{\text{size}}$ which favors larger independent sets. A naive weighted sum of both terms turned out to be unstable during training and yielded poor results, whereas the product in Equation (6) worked well. For training, \mathcal{L}_{MIS} is combined across iterations with a discount factor λ as in the standard RUN-CSP architecture.

We start by evaluating the performance on random graphs. We trained a network on 4,000 random Erdős-Rényi graphs with 100 nodes and $m \sim U(100, 600)$ edges each and with $\kappa = 1$. For evaluation we use random graphs with 100, 400, 800 and 1,600 nodes and a varying number of edges. For roughly 6% of all predictions, the predicted set contained induced edges (just a single edge in most cases), meaning the predicted sets were not independent. We corrected these predictions by removing one of the endpoints of each induced edge from the set and only report results after this correction. We compare RUN-CSP against two baselines: ReduMIS, a state-of-the-art MAX-IS solver (Akiba and Iwata 2016; Lamm et al. 2017) and a greedy heuristic, which we implemented ourselves. The greedy procedure iteratively adds the node with lowest degree to the set and removes the node and its neighbors from the graph until the graph is empty. Figure 3 shows the achieved independent set sizes, each data point is the mean IS size across 100 random graphs. For graphs with 100 nodes, RUN-CSP achieves similar sizes as ReduMIS and clearly outperforms the greedy heuristic. On larger graphs our network produces smaller sets than ReduMIS. However, RUN-CSP’s performance remains similar to the greedy baseline and, especially on denser graphs, outperforms it.

For more structured instances, we use a set of benchmark graphs from a collection of hard instances for combinatorial problems (Xu 2005). The instances are divided into five sets with five graphs each. These graphs were generated through the RB Model (Xu and Li 2003; Xu et al. 2005), a model for generating hard CSP instances. A graph of the class *frbc-k* consists of c interconnected k -cliques and the maximum independent set has a forced size of c . The previous model trained on Erdős-Rényi graphs did not perform well on these instances and produced sets with many induced edges. Thus, we trained a new network on 2,000 instances we generated ourselves through the RB Model. The exact generation procedure of this dataset is provided in the appendix. Training used a batch size of 5 for 25 epochs. We set $\kappa = 0.1$ to increase the importance of the independence condition. The predictions of the new model contained no induced edges for all benchmark instances. Table 5 contains the achieved IS sizes. RUN-CSP yields similar results as the greedy heuristic. While our network does not match the state-of-the-art heuristic, it still beats the greedy approach on instances with over 100,000 edges.

4. Conclusions

We have presented a universal approach for approximating MAX-CSPs with recurrent neural networks. Its key feature is the ability to train without supervision on any available data. Our experiments on the optimization problems MAX-2-SAT, MAX-CUT, 3-COL and MAX-IS show that RUN-CSP produces high quality approximations for all four

Table 5: Achieved IS sizes for the benchmark graphs. We report the mean and std. deviation for the 5 graphs in each group.

Graphs	$ V $	$ E $	RUN-CSP	Greedy	ReduMIS
frb30-15	450	18k	25.8 ± 0.8	24.6 ± 0.5	30 ± 0.0
frb40-19	790	41k	33.6 ± 0.5	33.0 ± 1.2	39.4 ± 0.5
frb50-23	1150	80k	42.2 ± 0.4	42.2 ± 0.8	48.8 ± 0.4
frb59-26	1478	126k	49.4 ± 0.5	48.0 ± 0.7	57.4 ± 0.9

problems. Our network can compete with traditional approaches like greedy heuristics or semi-definite programming on random data as well as benchmark instances. For MAX-2-SAT, RUN-CSP was able to outperform a state-of-the-art MAX-SAT Solver. Our approach also achieved better results than neural baselines, where those were available. RUN-CSP networks trained on small random instances generalize well to other instances with larger size and different structure. Our approach is very efficient and inference takes a few seconds, even for larger instances with over 10,000 constraints. The runtime scales linearly in the number of constraints and our approach can fully utilize modern hardware, like GPUs.

Overall, RUN-CSP seems like a promising approach for approximating MAX-CSPs with neural networks. The strong results are somewhat surprising, considering that our networks consist of just one LSTM Cell and a few linear functions. We believe that our observations point towards a great potential of machine learning in combinatorial optimization.

Future Work We plan to extend RUN-CSP to CSPs of arbitrary arity and to weighted CSPs. It will be interesting to see, for example, how it performs on 3-SAT and its maximization variant. Another possible future extension could combine RUN-CSP with traditional local search methods, similar to the approach by Li, Chen, and Koltun (2018) for MAX-IS. The soft assignments can be used to guide a tree search and the randomness can be exploited to generate a large pool of initial solutions for traditional refinement methods.

References

- [1] Martín Abadi et al. *TensorFlow: Large-Scale Machine Learning on Heterogeneous Systems*. Software available from tensorflow.org. 2015. URL: <http://tensorflow.org/>.
- [2] Ralph Abboud, Ismail Ilkan Ceylan, and Thomas Lukasiewicz. “Learning to Reason: Leveraging Neural Networks for Approximate DNF Counting”. In: *arXiv preprint arXiv:1904.02688* (2019).
- [3] Hans-Martin Adorf and Mark D Johnston. “A discrete stochastic neural network algorithm for constraint satisfaction problems”. In: *1990 IJCNN International Joint Conference on Neural Networks*. IEEE. 1990, pp. 917–924.
- [4] Takuya Akiba and Yoichi Iwata. “Branch-and-reduce exponential/FPT algorithms in practice: A case study of vertex cover”. In: *Theoretical Computer Science* 609 (2016), pp. 211–225.
- [5] Saeed Amizadeh, Sergiy Matushevych, and Markus Weimer. “Learning to solve circuit-SAT: An unsupervised differentiable approach”. In: *International Conference on Learning Representations* (2019). URL: <https://openreview.net/forum?id=BJxgz2R9t7>.
- [6] Josep Argelich. *Eleventh Evaluation of Max-SAT Solvers (Max-SAT-2016)*. 2016. URL: <http://maxsat.ia.udl.cat/introduction/>.
- [7] Fahiem Bacchus, Matti Järvisalo, and Ruben Martins. “MaxSAT Evaluation 2019: Solver and Benchmark Descriptions”. In: (2019).
- [8] Una Benlic and Jin-Kao Hao. “Breakout Local Search for the Max-Cut problem”. In: *Engineering Applications of Artificial Intelligence* 26.3 (2013), pp. 1162–1173. ISSN: 0952-1976. DOI: <https://doi.org/10.1016/j.engappai.2012.09.001>. URL: <http://www.sciencedirect.com/science/article/pii/S0952197612002175>.
- [9] Jeremias Berg, Emir Demirović, and Peter J Stuckey. “Core-boosted linear search for incomplete maxSAT”. In: *International Conference on Integration of Constraint Programming, Artificial Intelligence, and Operations Research*. Springer. 2019, pp. 39–56.
- [10] Stefan Boettcher and Allon G Percus. “Extremal optimization for graph partitioning”. In: *Physical Review E* 64.2 (2001), p. 026114.
- [11] Daniel Brélaz. “New methods to color the vertices of a graph”. In: *Communications of the ACM* 22.4 (1979), pp. 251–256.
- [12] Zhengdao Chen, Lisha Li, and Joan Bruna. “Supervised Community Detection with Line Graph Neural Networks”. In: *International Conference on Learning Representations*. 2019. URL: <https://openreview.net/forum?id=H1gOZ3A9Fm>.
- [13] Changhui Choi and Yinyu Ye. “Solving sparse semidefinite programs using the dual scaling algorithm with an iterative solver”. In: *Manuscript, Department of Management Sciences, University of Iowa, Iowa City, IA 52242* (2000).

- [14] Edward Dahl. “Neural network algorithms for an np-complete problem: map and graph coloring”. In: *Proc. First Int. Conf. Neural Networks III*. 1987, pp. 113–120.
- [15] Caterina De Simone et al. “Exact ground states of Ising spin glasses: New experimental results with a branch-and-cut algorithm”. In: *Journal of Statistical Physics* 80.1-2 (1995), pp. 487–496.
- [16] R. Dechter. *Constraint Processing*. Morgan Kaufmann, 2003.
- [17] Amir Dembo, Andrea Montanari, Subhabrata Sen, et al. “Extremal cuts of sparse random graphs”. In: *The Annals of Probability* 45.2 (2017), pp. 1190–1217.
- [18] Philippe Galinier and Jin-Kao Hao. “Hybrid evolutionary algorithms for graph coloring”. In: *Journal of combinatorial optimization* 3.4 (1999), pp. 379–397.
- [19] David W Gassen and Jo Dale Carothers. “Graph color minimization using neural networks”. In: *Proceedings of 1993 International Conference on Neural Networks (IJCNN-93-Nagoya, Japan)*. Vol. 2. IEEE. 1993, pp. 1541–1544.
- [20] Michel X Goemans and David P Williamson. “Improved approximation algorithms for maximum cut and satisfiability problems using semidefinite programming”. In: *Journal of the ACM (JACM)* 42.6 (1995), pp. 1115–1145.
- [21] Haidar Harmanani, Jean Hannouche, and Nancy Khoury. “A neural networks algorithm for the minimum colouring problem using FPGAs”. In: *International Journal of Modelling and Simulation* 30.4 (2010), pp. 506–513.
- [22] Federico Heras et al. “2006 and 2007 Max-SAT evaluations: Contributed instances”. In: *Journal on Satisfiability, Boolean Modeling and Computation* 4 (2008), pp. 239–250.
- [23] Demian Hesse, Christian Schulz, and Darren Strash. “Scalable kernelization for maximum independent sets”. In: *Journal of Experimental Algorithmics (JEA)* 24.1 (2019), pp. 1–22.
- [24] Petter Holme and Beom Jun Kim. “Growing scale-free networks with tunable clustering”. In: *Physical review E* 65.2 (2002), p. 026107.
- [25] John J Hopfield and David W Tank. ““Neural” computation of decisions in optimization problems”. In: *Biological cybernetics* 52.3 (1985), pp. 141–152.
- [26] Selman Kautz. *Walksat Home Page*. 2019. URL: <https://www.cs.rochester.edu/u/kautz/walksat/>.
- [27] Elias Khalil et al. “Learning combinatorial optimization algorithms over graphs”. In: *Advances in Neural Information Processing Systems*. 2017, pp. 6348–6358.
- [28] Sebastian Lamm et al. “Finding near-optimal independent sets at scale”. In: *Journal of Heuristics* 23.4 (2017), pp. 207–229.
- [29] Henrique Lemos et al. “Graph Colouring Meets Deep Learning: Effective Graph Neural Network Models for Combinatorial Problems”. In: *arXiv preprint arXiv:1903.04598* (2019).
- [30] Rhyd Lewis. *A guide to graph colouring*. Vol. 7. Springer, 2015.

- [31] Rhyd Lewis et al. “A wide-ranging computational comparison of high-performance graph colouring algorithms”. In: *Computers & Operations Research* 39.9 (2012), pp. 1933–1950.
- [32] Zhuwen Li, Qifeng Chen, and Vladlen Koltun. “Combinatorial optimization with graph convolutional networks and guided tree search”. In: *Advances in Neural Information Processing Systems*. 2018, pp. 539–548.
- [33] NetworkX developer team. *NetworkX*. 2014. URL: <https://networkx.github.io/>.
- [34] Marcelo Prates et al. “Learning to Solve NP-Complete Problems: A Graph Neural Network for Decision TSP”. In: *Proceedings of the AAAI Conference on Artificial Intelligence*. Vol. 33. 2019, pp. 4731–4738.
- [35] P. Raghavendra. “Optimal algorithms and inapproximability results for every CSP?” In: *Proceedings of the 40th ACM Symposium on Theory of Computing*. 2008, pp. 245–254.
- [36] Bart Selman, Henry A Kautz, Bram Cohen, et al. “Local search strategies for satisfiability testing.” In: *Cliques, coloring, and satisfiability* 26 (1993), pp. 521–532.
- [37] Daniel Selsam et al. “Learning a SAT Solver from Single-Bit Supervision”. In: *International Conference on Learning Representations*. 2019. URL: https://openreview.net/forum?id=HJMC_iA5tm.
- [38] Yoshiyasu Takefuji and Kuo Chun Lee. “Artificial neural networks for four-coloring map problems and K-colorability problems”. In: *IEEE Transactions on Circuits and Systems* 38.3 (1991), pp. 326–333.
- [39] Duncan J Watts. “Networks, dynamics, and the small-world phenomenon”. In: *American Journal of sociology* 105.2 (1999), pp. 493–527.
- [40] Ke Xu. *BHOSLIB: Benchmarks with Hidden Optimum Solutions for Graph Problems (Maximum Clique, Maximum Independent Set, Minimum Vertex Cover and Vertex Coloring)*. 2005. URL: <http://sites.nlsde.buaa.edu.cn/~kexu/benchmarks/graph-benchmarks.htm>.
- [41] Ke Xu and Wei Li. “Many hard examples in exact phase transitions with application to generating hard satisfiable instances”. In: *arXiv preprint cs/0302001* (2003).
- [42] Ke Xu et al. “A Simple Model to Generate Hard Satisfiable Instances”. In: *IJCAI-05, Proceedings of the Nineteenth International Joint Conference on Artificial Intelligence, Edinburgh, Scotland, UK, July 30 - August 5, 2005*. 2005, pp. 337–342. URL: <http://ijcai.org/Proceedings/05/Papers/0989.pdf>.
- [43] Weichi Yao, Afonso S Bandeira, and Soledad Villar. “Experimental performance of graph neural networks on random instances of max-cut”. In: *arXiv preprint arXiv:1908.05767* (2019).
- [44] Yinyu Ye. *The Gset Dataset*. 2003. URL: <https://web.stanford.edu/~yyye/Gset/>.

A. External Software and Data

Table 6 lists the versions and sources of all the external software used in our paper. Table 7 lists the sources of all the evaluation instances that we did not generate ourselves. All evaluation instances are also provided in our repository at <https://github.com/RUNCSP/RUN-CSP>

Table 6: Used Software

Software	Version	Author / Source
Tensorflow	1.15.2	(Abadi et al. 2015) https://tensorflow.org
NetworkX	2.4	(NetworkX developer team 2014) https://networkx.github.io
Loandra	2019	(Berg, Demirović, and Stuckey 2019) https://maxsat-evaluations.github.io/2019/descriptions
MaxWalkSAT	20	(Selman, Kautz, Cohen, et al. 1993) https://www.cs.rochester.edu/u/kautz/walksat/
ReduMIS	1.1	(Hespe, Schulz, and Strash 2019) http://algo2.iti.kit.edu/kamis/
HybridEA	2015	(Galinier and Hao 1999), (Lewis et al. 2012), (Lewis 2015) http://rhydlewis.eu/resources/gCol.zip
GNN-GCP	2020	(Lemos et al. 2019) https://github.com/machine-reasoning-ufrgs/GNN-GCP

Table 7: Used Data

Instances	Author / Source
Spinglass	(Heras et al. 2008)
2-CNF	http://maxsat.ia.udl.cat/benchmarks/ , Unweighted Crafted Benchmarks
Gset	(Ye 2003) https://www.cise.ufl.edu/research/sparse/matrices/Gset/
MAX-IS	(Xu 2005)
Graphs	http://sites.nlsde.buaa.edu.cn/~kexu/benchmarks/graph-benchmarks.htm

B. Reproducibility

This section summarizes the necessary information for replicating our implementation and exact training procedure. The information can also be found in training scripts provided in the source code. All trainable matrices in the messaging functions S_R were initialized with uniform Glorot initialization. For activation, bias, and initialization of the LSTM cell we used the default values provided by TensorFlow 1.14.0. All trainable parameters were regularized with the ℓ^2 -norm with a weight of 0.01. The pooled vectors of received messages $r_x^{(t)}$ were normalized with an additional batch normalization layer, before being passed into the LSTM cell. The discount factor in our loss function was set to $\lambda = 0.95$ in all experiments. The state size of all networks was set to $k = 128$.

All networks were trained with $t_{\max}^{\text{tr}} = 30$. Training was performed with the Adam optimizer using the default parameters $\beta_1 = 0.9$, $\beta_2 = 0.999$, and $\epsilon = 1 \times 10^{-7}$. The learning rate was initialized as 0.001 and decayed with a factor of 0.1 every 5 epochs. The gradients were clipped at a norm of 1.0.

B.1. Parallel execution

We perform 64 runs on each instance to boost the performance during evaluation. Our implementation performs these runs in parallel with a single forward pass of the network. To achieve this, we copy the graph 64 times and combine the disjoint copies into one larger instance. This instance is then processed by the RUN-CSP network. Since there are no messages exchanged between connected components, this is equivalent to executing the network 64 times on the same graph. Evaluating on a single large graph is, especially for small instances, faster on a GPU than multiple executions on the small graphs.

For the largest IS benchmark graphs the parallel inference with 64 copies exceeds the memory limit of our GPU. Instead, we performed 8 consecutive runs with 8 copies each and selected the best assignment afterwards.

C. Hard 3-Col Instances

Here, we describe how the ‘hard’ 3-col graphs used in our vertex coloring experiment are generated. These instances are 3-colorable Erdős-Rényi graphs and there is (at least) one edge e such that when adding e to the graph, it is non-3-colorable. To generate such a graph, we first initialize a graph with n nodes and no edges. We then iteratively add individual edges which are uniformly sampled at random. After adding each edge, we use a conventional SAT solver to check whether the graph is still 3-colorable. (We use the pycosat Python package for this task.) This process is stopped once the graph is found to be non-3-colorable. The graphs with and without the last added edge are then returned as negative and positive instances, respectively. Our graph generation procedure stops adding edges when the next randomly chosen edge makes the graph non-3-colorable. In contrast, Lemos et al. (2019) stopped adding edges when it was possible to add such an edge that makes the graph non-3-colorable. The graphs generated by Lemos et al. are thus less dense than ours.

D. Max-IS Benchmarks

The RUN-CSP network that was evaluated on the MAX-IS benchmark graphs was trained on our own synthetic benchmark instances. Here, we will describe the generation procedure of these instances. (Xu and Li 2003; Xu et al. 2005) proposed the RB Model, which is a general model for generating hard random CSP instances close to the phase change of satisfiability. Furthermore, they described how to generate hard instances for graph problems, including MAX-IS instances, by reducing SAT benchmarks of the RB Model to these problems. We used their generation procedure for MAX-IS benchmarks as described in Xu (2005). Given $c \in \mathbb{N}$, $p \in [0, 1]$ and $\alpha, r > 0$, the procedure generates a graph as follows:

1. Generate c disjoint cliques with $k = c^\alpha$ vertices each.
2. Select two random cliques and generate $pc^{2\alpha}$ random edges between them (without repetition).
3. Run Step 2 for another $rc \ln c - 1$ times (with repetition).

To enforce an optimal independent set of size c , one can exclude one node of each clique from the process of adding random edges.

We used this procedure to generate 2,000 training instances. For each graph we uniformly sampled $c \sim U(10, 25)$, $k \sim U(5, 20)$ and $p \sim U(0.3, 1.0)$. We then chose

$$\alpha = \frac{\ln(k)}{\ln(c)} \quad \text{and} \quad r = -\frac{\alpha}{\ln(1-p)} \quad (7)$$

This choice for r is expected to yield ‘hard’ instances according to the RB Model (Xu et al. 2005). We then used the algorithm described above to generate a graph with the chosen parameters.

Training was performed with a batch size of 5. Note that we reduced the batch size in comparison to all other experiments due to the relatively large size of the graphs. The constant κ that distributes the importance of the losses \mathcal{L}_{CSP} and $\mathcal{L}_{\text{size}}$ was reduced to $\kappa = 0.1$ to emphasize the independence condition. Without this reduction the computed solutions contained multiple edges violating independence and not just one or two as in the other IS experiment.

E. Additional Experiments

E.1. Detailed Gset Results

Table 8 provides the achieved cut sizes for additional Gset instances. As for the subset of instances provided in the Experiments Section, the RUN-CSP network performed 64 parallel evaluation runs with $t_{\text{max}}^{\text{ev}} = 500$ iterations.

Table 8: Achieved cut sizes on Gset instances for RUN-CSP, DSDP and BLS. The values for DSDP and BLS taken from the literature. DSDP values were only available for a subset of GSET.

Graph	type	$ V $	$ E $	RUN-CSP	DSDP	BLS
G1	<i>random</i>	800	19176	11369	-	11624
G2	<i>random</i>	800	19176	11367	-	11620
G3	<i>random</i>	800	19176	11390	-	11622
G14	<i>decay</i>	800	4694	2943	2922	3064
G15	<i>decay</i>	800	4661	2928	2938	3050
G16	<i>decay</i>	800	4672	2921	-	3052
G22	<i>random</i>	2000	19990	13028	12960	13359
G23	<i>random</i>	2000	19990	13006	13006	13344
G24	<i>random</i>	2000	19990	13001	12933	13337
G35	<i>decay</i>	2000	11778	7339	-	7684
G36	<i>decay</i>	2000	11766	7325	-	7678
G37	<i>decay</i>	2000	11785	7317	-	7689
G48	<i>torus</i>	3000	6000	6000	6000	6000
G49	<i>torus</i>	3000	6000	6000	6000	6000
G50	<i>torus</i>	3000	6000	5880	5880	5880
G51	<i>decay</i>	1000	5909	3690	-	3848
G52	<i>decay</i>	1000	5916	3681	-	3851
G53	<i>decay</i>	1000	5914	3695	-	3850
G55	<i>random</i>	5000	12468	10116	9960	10294

E.2. Structure Specific Performance for Max-3-Col

A key feature of RUN-CSP is the unsupervised training procedure, which allows us to train a network on arbitrary data without knowledge of any optimal solutions. Intuitively, we would expect a network trained on instances of a particular structure to adapt toward this class of instances and perform poorer for different structures. We will briefly evaluate this hypothesis for four different classes of graphs using the MAX-3-COL problem.

Erdős-Rényi Graphs: Graphs are generated by uniformly sampling m distinct edges between n nodes.

Geometric Graphs: A graph is generated by first assigning random positions within a 1×1 square to n distinct nodes. Then an edge is added for every pair of points with a distance less than r .

Powerlaw-Cluster Graphs: This graph model was introduced by Holme and Kim (2002). Each graph is generated by iteratively adding n nodes. Every new node is connected to m random nodes that were already inserted. After each edge is added, a triangle is closed with probability p , i.e. an additional edge is added between the inserted node and a random neighbor of the other endpoint of the edge.

Regular Graphs: We consider random 5-regular graphs as an example for graphs with very specific structure class.

For each graph class we generated a training dataset with 4,000 random instances. The number of nodes was sampled uniformly between 50 and 100 for each graph of all four classes. For Erdős-Rényi graphs, the edge count m was chosen randomly between 100 and 400. The parameter r of each geometric graph was sampled uniformly from the interval $[0.1, 0.2]$. For Powerlaw-Cluster graphs, the parameter m was uniformly sampled from $\{1, 2, 3\}$ and p was uniformly drawn from the interval $[0, 1]$. Five RUN-CSP models were trained on each dataset. We refer to these groups of models as M_{ER} , M_{Geo} , M_{Pow} and M_{Reg} . Additionally, 5 models M_{Mix} were trained on a mixed dataset with 1,000 random instances of each graph class.

For evaluation, we generated 1,000 instances of each class. Table 9 contains the percentage of unsatisfied constraints over the models and graph classes. In general, all models perform well on the class of structures they were trained on. M_{Geo} and M_{Pow} outperform M_{ER} on Erdős-Rényi graphs while M_{ER} outperforms M_{Geo} on Powerlaw-Cluster graphs and M_{Pow} on geometric graphs. The networks trained on 5-regular graphs only perform well on the same class and yield poor results for other structures. Overall, M_{Mix} produced the best results when averaged over all four classes, despite not achieving the best results for any particular class.

E.3. Detailed 3-Col Results

In Section 3.3 of the main paper we evaluated RUN-CSP on the 3-COL problem for hard random instances. There, the models were trained on hard 3-colorable instances. To further evaluate how the training data effects RUN-CSP models, we also applied networks trained on different datasets to the same hard evaluation instances. We trained five networks on the negative non-3-colorable counterparts of the positive training instances used earlier. Furthermore, we applied the five models of M_{Mix} from the previous section to the hard evaluation instances. The achieved percentages of optimally 3-colored graphs are provided in Table 10.

Table 9: Percentages of unsatisfied constraints for each graph class under the different RUN-CSP models. Values are averaged over 1,000 graphs and the standard deviation is computed with respect to the five RUN-CSP models.

Graphs	M_{ER} (%)	M_{Geo} (%)	M_{Pow} (%)	M_{Reg} (%)	M_{Mix} (%)
Erdős-Rényi	4.75 ± 0.01	4.73 ± 0.02	4.72 ± 0.02	6.69 ± 1.60	4.73 ± 0.01
Geometric	10.33 ± 0.07	10.16 ± 0.04	11.39 ± 0.66	18.99 ± 3.32	10.18 ± 0.03
Pow. Cluster	1.89 ± 0.00	1.96 ± 0.01	1.87 ± 0.00	2.44 ± 0.67	1.89 ± 0.00
Regular	2.33 ± 0.01	2.41 ± 0.03	2.33 ± 0.02	2.32 ± 0.00	2.33 ± 0.00
Mean	4.83 ± 0.02	4.82 ± 0.03	5.08 ± 0.18	7.61 ± 1.40	4.78 ± 0.01

Table 10: Percentages of hard positive instances for which optimal 3-colorings were found by different RUN-CSP models, Greedy Search (DSatur), and HybridEA. The RUN-CSP models were trained on only positive (Pos.), only negative instances (Neg.), or the mixed random graphs from the previous experiment. We report mean and standard deviation across five RUN-CSP models that were trained on each dataset.

Nodes	RUN-CSP (Pos.)	RUN-CSP (Neg.)	RUN-CSP (M_{Mix})	Greedy	HybridEA
50	98.4 ± 0.3	98.7 ± 0.3	97.4 ± 0.5	34.0	100.0
100	62.5 ± 2.7	58.9 ± 3.0	43.2 ± 2.5	6.7	100.0
150	15.5 ± 2.3	14.1 ± 1.7	6.7 ± 0.4	1.5	98.7
200	2.6 ± 0.4	1.9 ± 0.3	0.5 ± 0.3	0.5	88.9
300	0.1 ± 0.0	0.2 ± 0.1	0.1 ± 0.1	0.0	39.9
400	0.0 ± 0.0	0.0 ± 0.0	0.0 ± 0.0	0.0	15.3

On graphs with over 50 nodes the models trained on negative hard instance perform marginally worse than those trained on the positive counterparts. The models of M_{Mix} perform worse than those trained on hard instances, especially for the larger graphs. However, they do still outperform the traditional greedy heuristic by a significant margin.

E.4. Convergence of RUN-CSP

We now use the MAX-3-COL problem to illustrate the convergence behavior of RUN-CSP networks. We generated a random Erdős-Rényi graph with 500 nodes and 2,000 edges. One of the RUN-CSP models of M_{Mix} from the previous experiment was used to predict a maximum 3-coloring for this graph. We performed 64 parallel evaluation runs for $t_{\text{max}}^{\text{ev}} = 100$ iterations. For each iteration we obtain 64 values for the numbers of correctly colored edges, one for each parallel run. Figure 4 plots the distributions of these values across all iterations as boxplots. In the first 20 time steps, the predictions improve quickly, as the network moves away from its random initialization towards a better solution. The network continues to find better color assignments far past iteration 30, which is the number iterations used during training, the absolute maximum was reached in iteration 67.

E.5. Coloring Benchmark Instances

We evaluated RUN-CSP on a number of k -COL benchmark instances, similar to Lemos et al. (2019). We obtained the 20 graphs from the COLOR02 Workshop² that were also used to evaluate GNN-GCP to enable a direct comparison. Any single RUN-CSP network is bound to a fixed domain size d . A network cannot use more than d colors and even if a given graph can be colored with less than d colors, RUN-CSP will still use all d colors. Thus, in order to compute a chromatic number, we trained 14 distinct networks with domain sizes ranging from 4 to 17. We apply each network to a given graph and

²The graphs can be downloaded at <https://mat.tepper.cmu.edu/COLOR02/>

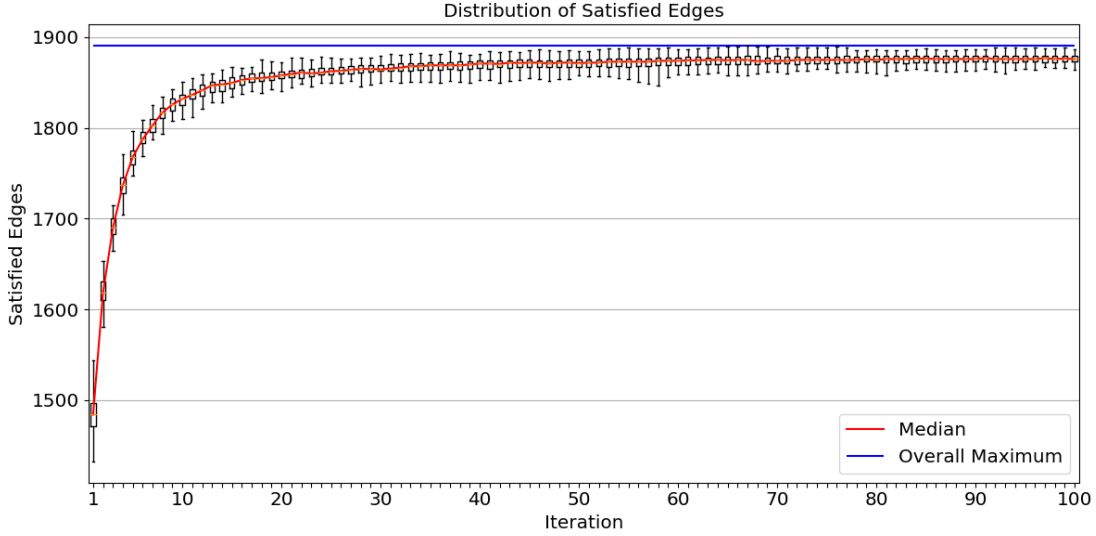


Figure 4: The distribution of satisfied edges for 64 parallel evaluation runs on a random Erdős-Rényi graph. For each iteration we show a boxplot that represents the 64 numbers of satisfied edges at a given time step. The whiskers of the boxplots include the minimum and maximum values. The limits of the box are given by the upper and lower quartile. The red line represents the median in each iteration. The overall maximum (reached after 67 steps) is shown as a horizontal blue line.

choose the output that achieved a conflict free coloring with the fewest colors as our final result.

Unlike our experiments for MAX-CUT, we found that RUN-CSP networks trained purely in Erdős-Rényi graphs performed poorly in the given setup. Instead, we generated mixed datasets that consist of 30% Erdős-Rényi graphs, 30% Geometric graphs, 30% Powerlaw-Cluster graphs and 10% Connected Caveman graphs (Watts 1999). Connected Caveman graphs are a graph model introduced by Watts (1999) that depends on two numbers $l, k \in \mathbb{N}$. All other graph classes were introduced in the Section 5.2.

The training datasets were adapted to the number $c \in \{4, \dots, 17\}$ of colors available such that networks with more colors were trained on denser graphs. Each training set contained 4,000 random graphs generated according to the following parameters:

Erdős-Rényi: $n \sim U(50, 100)$, $m \sim U(2n, n \cdot c)$

Geometric: $n \sim U(80, 28c)$, $r \sim U(0.1, 0.2)$

Powerlaw-Cluster: $n \sim U(20, 20c)$, $m \sim U(1, 4)$, $r \sim U(1, 2)$

Connected Caveman: $l \sim U(10, 20)$, $k \sim U(\max(4, c - 2), c + 2)$

We compare RUN-CSP to the classical methods used in our previous vertex coloring experiment, namely HybridEA and the greedy DSatur strategy. As before, HybridEA

Table 11: Results for k -COL on benchmarks instances. We provide the number of colors needed for an optimal coloring by RUN-CSP, Greedy (DSatur) and HybridEA. For GNN-GCP we provide the prediction as reported by Lemos et al. (2019). This method only predicts the chromatic number and can therefore underestimate the true value.

Benchmark	$ V $	Opt	RUN-CSP	GNN-GCP	DSatur	HybridEA
Queen5_5	25	5	5	6	5	5
Queen6_6	36	7	8	7	8	7
myciel5	47	6	6	5	6	6
Queen7_7	49	7	10	8	9	7
Queen8_8	64	9	11	8	10	9
1-Insertions_4	67	4	5	4	5	5
huck	74	11	11	8	11	11
jean	80	10	10	7	10	10
Queen9_9	81	10	17	9	12	10
david	87	11	11	9	11	11
Mug88_1	88	4	4	3	4	4
myciel6	95	7	8	7	7	7
Queen8_12	96	12	17	10	13	12
games120	120	9	9	6	9	9
Queen11_11	121	11	> 17	12	15	12
anna	138	11	11	11	11	11
2-Insertions_4	149	4	5	4	5	5
Queen13_13	169	13	> 17	14	17	14
myciel7	191	8	9	NA	8	8
homer	561	13	17	14	13	13

was allowed to perform 500 million constraint checks on each graph. Table 11 provides the number of colors that each method needed to color the graphs without conflict. For comparison, we provide the predicted chromatic number of GNN-GCP as reported by Lemos et al. (2019). On most benchmark instances HybridEA finds the optimal chromatic number and otherwise uses one additional color. For instances with a chromatic number of up to 6 the performance of our network is identical to DSatur and HybridEA. In general, RUN-CSP performs slightly worse than the greedy DSatur algorithm. The number of instances for which RUN-CSP found optimal solutions is larger than the number of graphs for which GNN-GCP predicted the correct chromatic number. We point out that the focus of our architecture is a maximization task associated with a domain of fixed size. Despite this, RUN-CSP was able to outperform GNN-GCP on this task, while also predicting color assignments.